Ring finger protein 215 is a potential prognostic biomarker involved in immune infiltration and angiogenesis in colorectal cancer

JING-BO WU[1], XIAO-JING LI[1], HUI LIU[1] and XIU-PING LIU[2]

[1]Department of Pathology, Shanghai Fifth People's Hospital, Fudan University, Shanghai 200240;
[2]Department of Pathology, School of Basic Medical Sciences, Fudan University, Shanghai 200032, P.R. China

Abstract. The prognostic value of ring finger protein 215 (RNF215) in colorectal cancer (CRC) is unclear. Herein, the present study aimed to investigate the precise value of RNF215 based on CRC datasets from The Cancer Genome Atlas (TCGA) and clinical cases. CRC patient data was collected from TCGA and clinical samples from the Department of Pathology, Shanghai Fifth People's Hospital, Fudan University (Shanghai, China). Logistic regression analysis was used to investigate the correlations between RNF215 and clinicopathological characteristics. The predictive value of RNF215 for the clinical outcome of CRC was determined using Kaplan-Meier curves and Cox regression. Gene set enrichment analysis (GSEA), single-sample GSEA (ssGSEA), and angiogenesis analysis were also conducted to investigate the biological role of RNF215. Immunohistochemistry was conducted to validate the results. The results of the present study confirmed that RNF215 protein expression was significantly associated with age, lymphatic invasion, and overall survival (OS). Univariate analysis showed that upregulation of RNF215 in CRC was significantly associated with age and lymphatic invasion. Kaplan-Meier survival analysis revealed that high RNF215 expression predicted poorer OS and disease-specific survival. A total of nine experimentally detected RNF215-binding proteins were identified with the STRING tool and Cytoscape software. GSEA suggested that RNF215 was associated with several important pathways involved in tumor occurrence, including the Kyoto Encyclopedia of Genes and Genomes MAPK signaling pathway and the WikiPathway RAS signaling pathway. ssGSEA confirmed that RNF215 was significantly expressed in natural killer cells, CD8 T cells and T helper cells. Angiogenesis analysis revealed that numerous angiogenesis-related genes had the same expression trend as RNF215 in CRC. The immunostaining results indicated that RNF215 expression was significantly higher in CRC tissues than in corresponding normal tissues. In conclusion, increased RNF215 expression may be a potential molecular marker predictive of poor survival and a treatment target in CRC. In addition, RNF215 may participate in the formation of CRC through a variety of signaling pathways.

Correspondence to: Dr Jing-Bo Wu, Department of Pathology, Shanghai Fifth People's Hospital, Fudan University, 801 Heqing Road, Shanghai 200240, P.R. China
E-mail: wujingbo@fudan.edu.cn

Abbreviations: AUC, area under the curve; ACC, adrenocortical carcinoma; BLCA, bladder cancer; BP, biological process; CC, cellular component; CHOL, cholangiocarcinoma; COAD, colon adenocarcinoma; CRC, colorectal cancer; DEG, differentially expressed gene; DSS, disease-specific survival; FC, fold change; FDR, false discovery rate; FFPE, formalin-fixed paraffin-embedded; GEO, Gene Expression Omnibus; GO, Gene Ontology; GSEA, gene set enrichment analysis; IHC, immunonohistochemistry; C-index, concordance index; KEGG, Kyoto Encyclopedia of Genes and Genomes; MF, molecular function; NES, normalized enrichment score; OS, overall survival; PFI, progression-free interval; PPI, protein-protein interaction; RNF215, ring finger protein 215; ROC, receiver operating characteristic; ssGSEA, single-sample gene set enrichment analysis; TCGA, The Cancer Genome Atlas; TMA, tissue microarray

Key words: ring finger protein 215, colorectal cancer, prognostic biomarker, The Cancer Genome Atlas, immunohistochemistry

Introduction

Colorectal cancer (CRC) is one of the most prevalent malignant tumors in the world. Approximately 19 million new cases and 10 million cancer-related deaths were estimated in 2020 (1,2). It has also been estimated that in 2015, there were 376,000 new CRC patients and 190,000 CRC-related deaths in China (3). Although great efforts have been made to improve the early diagnosis and treatment of CRC, including advances in screening tools, surgical treatment, chemotherapy, and targeted biologic therapy, a large proportion of patients with advanced CRC still have a poor prognosis (4,5). The 5-year survival rate of early-stage CRC patients is ~90%, while it drops to 13.1% for patients with advanced CRC (6). Since CRC presents symptoms only at an advanced stage, the morbidity and mortality of CRC can be expected to be reduced by early screening programs. Considering this, the American

Cancer Society has revised its guidelines for individuals with an average CRC risk, lowering the screening age from 50 to 45 years (7). Given the limitations of CRC screening, such as its invasiveness, high expense, and low sensitivity and specificity, it is important to explore new early screening molecular markers and potential therapeutic targets with predictive or prognostic value for CRC.

According to GeneCards (https://www.genecards.org/cgi-bin/carddisp.pl?gene=RNF215), ring finger protein 215 (RNF215) is a multichannel membrane protein containing a ring-finger type zinc finger with 377 amino acids, 9 exons, and a molecular mass of 41101 Da. The gene is a protein-coding gene located on 22q12.2, and an important paralog of this gene is RNF128. To date, only a few studies have been conducted on the RNF215 protein. Wu *et al* (8) reported that RNF215 interacts with p65 to reduce the production of type I interferons (IFNs); thus, it is considered to be a key negative regulator of type I IFNs and has been considered a potential target for disease intervention with aberrant IFN production. Ma *et al* (9) suggested that high RNF215 expression is associated with poor overall survival (OS), demonstrating its function as a head and neck cancer (HNSC) oncogene. McIntosh *et al* performed quantitative trait locus (QTL) expression analysis, which showed that the single-nucleotide polymorphism (SNP) variations near RNF215 were correlated with the expression levels of the neighboring gene MTP18/SF3A1 (10).

However, the association between RNF215 and CRC has not been reported, and the exact role of RNF215 in the prognosis and biological function of CRC has not been identified. Therefore, the association between RNF215 and CRC was evaluated and the possible role of RNF215 in CRC prognosis was analyzed through datasets obtained from The Cancer Genome Atlas (TCGA). The difference in RNF215 expression between CRC tumor and normal tissues was investigated by analyzing the RNA sequencing (RNA-seq) data of CRC tumors. Subsequently, the association between RNF215 expression and CRC clinicopathological characteristics as well as prognosis was investigated. Furthermore, gene set enrichment analysis (GSEA) was conducted to confirm the functional pathways correlated with RNF215 in CRC. Immune infiltration and angiogenesis were then examined to analyze their association with RNF215, and the possible mechanism of RNF215 involvement in CRC was investigated. Finally, the findings of the present study were validated using immunohistochemistry (IHC) on samples from patients with CRC obtained from the Department of Pathology, Shanghai Fifth People's Hospital, Fudan University (Shanghai, China). The present research demonstrated, to the best of our knowledge for the first time, not only the importance of RNF215 but also its potential roles as a molecular prognostic marker for prognosis and as a therapeutic target in CRC.

Materials and methods

Data collection. RNF215 expression and clinical data of pancancer and CRC cohorts were collected from TCGA (https://cancergenome.nih.gov/). The normalized RNA-seq data and associated clinicopathological data of 647 CRC tumor tissues and 51 normal tissues were also collected from the TCGA database. The RNA-seq gene expression data in transcripts per million reads (TPM) with CRC and clinical information were further analyzed. The present study was conducted following the public guidelines provided by TCGA. In addition, a total of 177 CRC patient tissues and paired normal tissue samples were obtained from the Department of Pathology, Shanghai Fifth People's Hospital, Fudan University, between January 2012 and December 2016. A total of 116 males and 61 females, with a median age at diagnosis of 67 years (range, 33-95 years) were included in the present study. The inclusion criteria for patients with CRC were as follows: i) All of the patients with pathological and imaging examinations who met the CRC diagnostic standards; ii) patients who had no family history of CRC; and iii) patients who had good mental health. The exclusion criteria were as follows: i) patients who did not meet the diagnostic standards of CRC; ii) patients who were diagnosed with serious heart, lung, and other important organ diseases; and iii) patients who were not conscious or were unable to communicate normally. The research was conducted with approval from the Ethics Committee of Shanghai Fifth People's Hospital, Fudan University (approval no. 2021071). The study was performed according to the flowchart in Fig. 1.

CRC differentially expressed gene (DEG) analysis. Based on the median RNF215 expression level of TCGA CRC patients, the patients were classified into two groups (the low-expression group and high-expression group). A comparison of the expression profile (HTSeq-TPM) of RNF215 between the two groups and identification of DEGs were conducted with the R limma package (11). Genes with a $\log_2$|fold change (FC)|>1.5 and a false discovery rate (FDR) <0.05 were identified as DEGs.

Functional enrichment analysis. To clarify the potential function of RNF215, the R package DESeq2 was used to identify the differences between the two groups (high vs. low RNF215 expression) (12) by setting the thresholds to a $\log_2$|FC|>1.5 and an adjusted P-value (P.adj) <0.05. Gene Ontology (GO) and Kyoto Encyclopedia of Genes and Genomes (KEGG) enrichment analyses were conducted using the R packages clusterProfiler and ggplot2 (13). GO and KEGG analyses combined with logFC enrichment analysis was conducted with the R packages GOplot and ggplot2 (14).

GSEA. GSEA (https://gseamsigdb.org) is a type of genome analysis method used for interpretation of gene expression data (15). In order to clarify the potential functions of RNF215, GSEA was conducted with the R package clusterProfiler (version, 3.14.3) to investigate the positive functional and pathway differences between the high- and low-RNF215-expression groups (13). Among the Molecular Signature Database (MSigDB) collections, c2.cp.v7.0.symbols.gmt [Curated] was used as the reference gene set. The RNF215 expression value was selected as a marker of phenotype. Pathway enrichment was performed under the following conditions: P.adj <0.05, FDR <0.25, and normalized enrichment score (NES) >1. STRING tools (https://cn.string-db.org/) and Cytoscape software (version, 3.9.1) were used to build the protein-protein interaction (PPI) network (16-18).
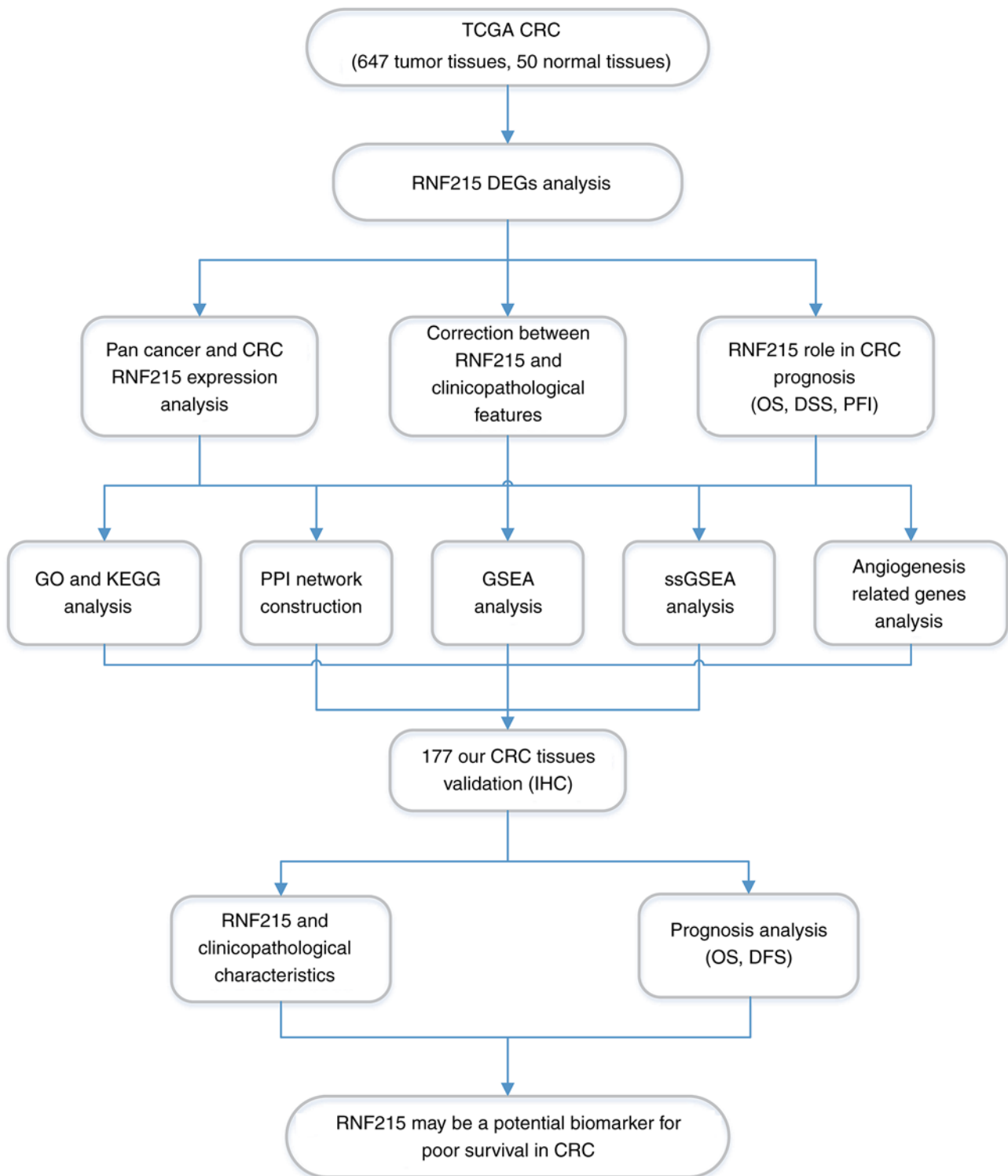
Figure 1. Flowchart of the study. The study was performed according to the flowchart.

Single-sample GSEA (ssGSEA). The ssGSEA method was used with the R package GSA (version, 1.34.0) to analyze CRC tumor tissues for the infiltration of 24 immune cell species (19). According to the marker genes of the 24 types of immunocytes (20), the relative enrichment fraction was calculated based on the gene expression profile in tumor tissue. Spearman's correlation analysis was used to confirm the correlation between RNF215 and immune cells. Detection of immune cell infiltration was performed with the Wilcoxon rank sum test.

Immunohistochemistry (IHC). A tissue microarray (TMA) was constructed using all 177 formalin-fixed paraffin-embedded (FFPE) CRC tumor tissues, and each tumor tissue consisted of three representative 1.5 mm punches, as described in a previous study by the authors (21). All tissues were fixed with 10% formalin at room temperature (20°C) for more than 24 h. Antigen retrieval was performed with a pressure cooker (Y-60C816, Joyoung, Hangzhou, China) for 30 min at 100°C. To block

endogenous peroxidase, the slides were immersed in 3% hydrogen peroxide for 10 min at 20˚C.

TMA slides (3-*μ*m thick) were automatically immunized with a Ventana benchmark instrument (Roche Diagnostics) following the manufacturer's instructions. Slides were incubated with a primary antibody for 14 h at 4˚C followed by the application of a secondary antibody [ultraView Universal HRP Multimer (55 *μ*g/ml); cat. no. (92)760-500; Ventana Medical Systems, Inc.] for 40 min at 37˚C. Finally, 3,3'-diaminobenzidine (DAB) was used as the chromogenic substrate and slides were counterstained with hematoxylin for 1 min at 20˚C. Commercially available antibodies against RNF215 (polyclonal; 1:300; product no. Ys-9264R; Shanghai YaJi Biotechnology Co., Ltd.) and CD34 (clone EPR2999; cat. no. ab110643; 1:150; Abcam) were used for IHC. Appropriate positive and negative control slides were included for each antibody. All CRC images subjected to hematoxylin and eosin (H&E) staining and IHC were viewed under a light microscope (BX45; Olympus Corporation).

All immunostaining results were evaluated by two gastrointestinal pathologists (JBW and XPL). The presence of a brown color in the cytoplasm and membrane was considered positive labeling. According to IHC evaluation methods adapted from previous studies (22), the presence and degree of RNF215 staining were divided into three categories: Negative expression, weak expression, and overexpression. The chi-square test or Fisher's test was conducted to identify the association between RNF215 expression and clinicopathological characteristics.

Statistical analysis. Statistical analyses were conducted with R software (version, 3.6.3) and Graph Prism (version, 9.0; GraphPad Software, Inc.; Dotmatics). The Wilcoxon rank sum test was used to compare the expression of RNF215 in CRC tumors with that in normal tissues. The Wilcoxon rank sum/Kruskal-Wallis test and logistic regression were performed to demonstrate the association between CRC clinicopathological characteristics and RNF215 expression. The CRC clinicopathological features correlated with survival were analyzed using the Kaplan-Meier method and Cox regression (23). Multivariate Cox analysis was conducted to assess the effect of RNF215 expression and the other clinicopathological features on survival. The variables with P<0.1 in univariate Cox regression analysis were further assessed in multivariate Cox regression analysis. Two-sided P-values <0.05 were considered to indicate a statistically significant difference.

Results

Pancancer and CRC RNF215 expression analysis. First, RNF215 expression was evaluated based on TCGA pancancer data. The results indicated that RNF215 expression was higher in 13 types of tumors than in their paired normal tissues, including bladder carcinoma (BLCA), breast invasive carcinoma (BRCA), cholangiocarcinoma (CHOL), colon adenocarcinoma (COAD), esophageal carcinoma (ESCA), HNSC, kidney renal clear cell carcinoma (KIRC), liver hepatocellular carcinoma (LIHC), lung adenocarcinoma (LUAD), lung squamous cell carcinoma (LUSC), prostate

adenocarcinoma (PRAD), rectal adenocarcinoma (READ), and stomach adenocarcinoma (STAD) (all P<0.05; Fig. 2A). Second, RNF215 expression in 647 CRC samples and 51 paracancerous samples as well as 50 CRC samples and their paired paracancerous samples were compared. RNF215 was overexpressed in CRC samples compared with paracancerous tissues (P<0.001; Fig. 2B and C). The area under the receiver operating characteristic (ROC) curve (AUC) was 0.845 (95% CI, 0.794-0.896; P<0.001), which showed that RNF215 had high diagnostic accuracy for CRC (Fig. 2D).

The abbreviations of TCGA cancers used in the present study and their paired full names are displayed in Table SI.

DEG analysis in CRC. DEG analysis was conducted using cohort data from TCGA. Based on the RNF215 expression level, the CRC patients were classified into high and low expression groups. A total of 431 DEGs were identified by screening, among which 145 were upregulated and 286 were downregulated (Fig. 3A). A heatmap of gene expression was constructed and the top 10 positive and 10 negative genes that had the greatest expression differences in CRC were obtained (Fig. 3B).

Association of RNF215 expression and clinicopathological characteristics in CRC. A total of 644 primary CRC specimens with clinical and RNF215 expression data were obtained from TCGA. There were 343 males and 301 females in the cohort with median ages of 69 and 66 years, respectively. Significant differences were identified between the high- and low-RNF215-expression groups in age (P=0.001), lymphatic invasion (P=0.017), and OS (P=0.018; Table SII). No other positive associations were identified between RNF215 expression and other clinicopathological characteristics. Univariate logistic regression analysis indicated that the upregulation of RNF215 in CRC was positively correlated with age (P<0.001) and lymphatic infiltration (P=0.014) but not with other clinicopathological features, as shown in Table I.

As indicated in Fig. 4, high RNF215 expression was positively correlated with age (P<0.001), tumor presence (P<0.001), lymphatic invasion (P<0.05), and OS event (P<0.01).

Prognostic role of RNF215 in CRC patients. To further identify the association between RNF215 expression and CRC prognosis, the survival rates of the high- and low-RNF215-expression groups were compared. Kaplan-Meier survival analysis indicated that patients with high RNF215 expression had poorer OS [median, 20.70 months vs. 24.33 months; HR=1.64 (1.15-2.33); P=0.006], poorer disease-specific survival [DSS; median, 19.97 months vs. 23.93 months; HR=1.69 (1.07-2.66); P=0.023], and a shorter progression-free interval [PFI; median, 17.80 months vs. 20.07 months; HR=1.27 (0.94-1.73); P=0.125], although the PFI difference was not significant (Fig. 5). T stage, N stage, pathological stage, age, primary therapy outcome, residual tumor, CEA level, lymphatic invasion, and RNF215 expression were included in the multivariate Cox analysis. Multivariate analysis revealed that RNF215 remained independently associated with OS [HR=1.859 (1.254-2.755), P=0.002], as well as other characteristics; the details are presented in Table II.
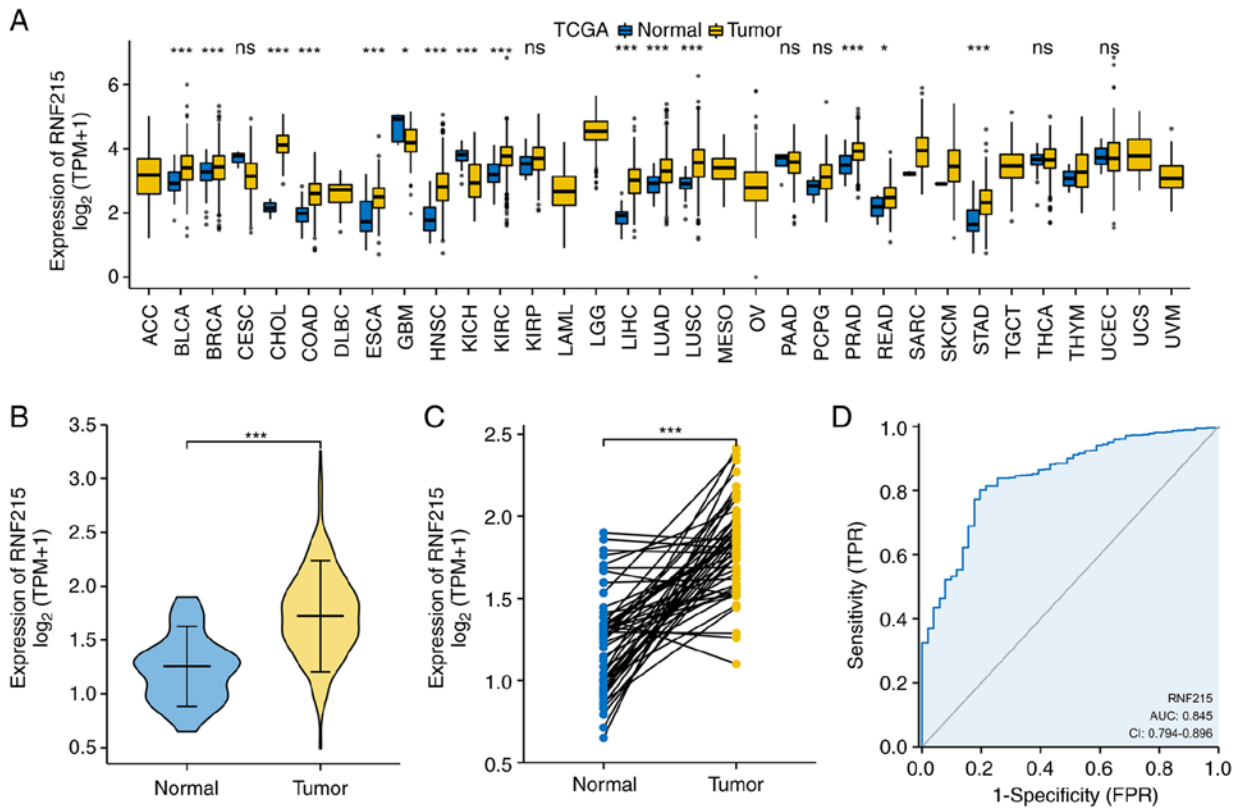
Figure 2. Differential expression map of RNF215. (A) Differential expression of RNF215 in tumor and normal tissues in 33 different cancer types from TCGA data. (B) RNF215 expression in normal and tumor tissues in CRC cases from TCGA. (C) Expression of RNF215 in CRC tumor tissues and paired normal tissues in TCGA. (D) Receiver operating characteristic curve showing the efficiency of RNF215 in predicting CRC. *P<0.05 and ***P<0.001. RNF215, ring finger protein 215; TCGA, The Cancer Genome Atlas; CRC, colorectal cancer; ns, not significant.
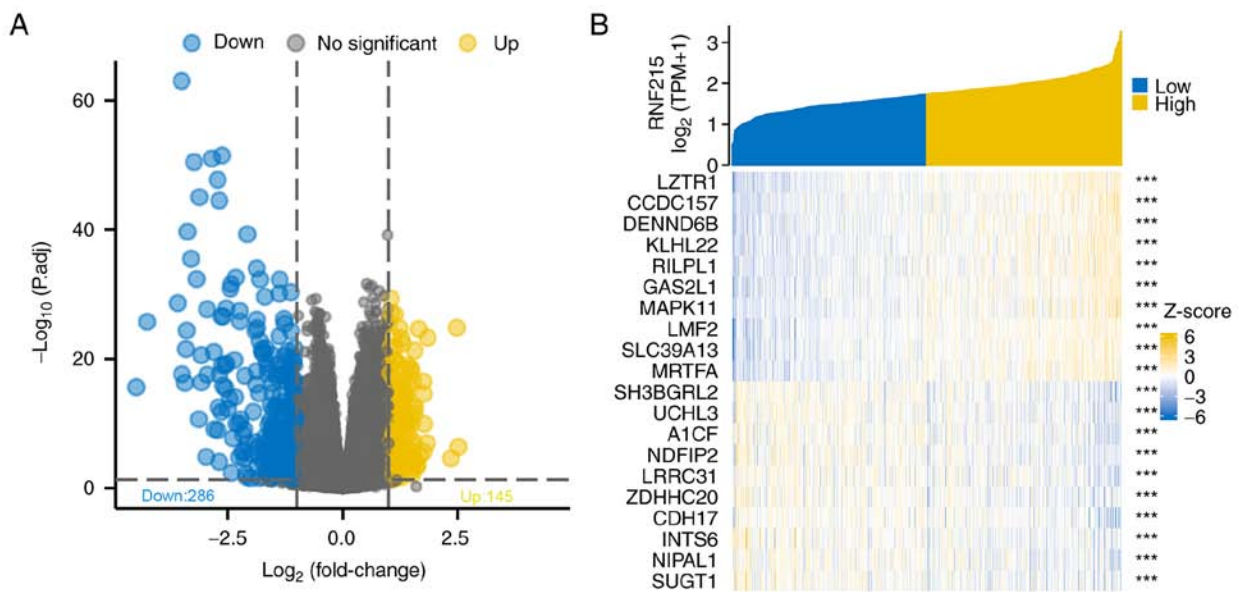

Figure 3. Differential expression genetic map of colorectal cancer in The Cancer Genome Atlas database. (A) Volcano plot. The y-axis is the logarithm of-log10 (P.adj). The larger the value, the more significant the difference. The x-axis is the $\log_2$(FC) value, and a larger absolute value indicates a greater fold change. Among all the 431 DEGs, 145 were upregulated and 286 were downregulated. (B) A heatmap of top 10 upregulated and top 10 downregulated DEGs. Each column represents a sample and each row represents one gene. Yellow represents high expression, and blue represents low expression. ***P<0.001. DEGs, differentially expressed genes; RNF215, ring finger protein 215.

Based on the results of the Cox proportional hazards regression model, T stage, N stage, M stage, TP53 status, age, lymphatic invasion, and RNF215 expression were selected for inclusion in the nomogram (Fig. 6A). The concordance index (C-index) of the prognostic model was 0.777 (0.752-0.803). A calibration plot of the nomogram-predicted survival

Table I. Ring finger protein 215 expression is associated with pathological characteristics (logistic regression) in colorectal cancer.

| Characteristics	Total (N)	Odds ratio (OR)	P-value
T stage (T3 and T4 vs. T1 and T2)	641	0.905 (0.616-1.329)	0.610
N stage (N1 and N2 vs. N0)	640	1.136 (0.831-1.556)	0.424
M stage (M1 vs. M0)	564	1.153 (0.733-1.818)	0.539
Pathologic stage (stage III and IV vs. stage I and II)	623	1.149 (0.838-1.578)	0.389
Primary therapy outcome (PR and CR vs. PD and SD)	312	1.260 (0.637-2.538)	0.510
Sex (male vs. female)	644	0.894 (0.655-1.218)	0.477
Race (Black or African American and White vs. Asian)	394	1.076 (0.331-3.497)	0.900
Age (>65 vs. ≤65)	644	0.585 (0.426-0.801)	<0.001
Weight (>90 vs. ≤90)	348	0.896 (0.566-1.420)	0.641
Height (≥170 vs. <170)	329	1.082 (0.701-1.669)	0.722
BMI (≥25 vs. <25)	329	0.960 (0.604-1.524)	0.862
Residual tumor (R1 and R2 vs. R0)	510	1.471 (0.779-2.839)	0.239
CEA level (>5 vs. ≤5)	415	0.915 (0.614-1.363)	0.661
Perineural invasion (yes vs. no)	235	1.292 (0.717-2.355)	0.396
Lymphatic invasion (yes vs. no)	582	1.522 (1.091-2.128)	0.014
History of colon polyps (yes vs. no)	555	1.027 (0.719-1.467)	0.884
Colon polyps present (yes vs. no)	323	1.250 (0.778-2.016)	0.357
Location (colon vs. rectum)	644	0.878 (0.616-1.250)	0.471
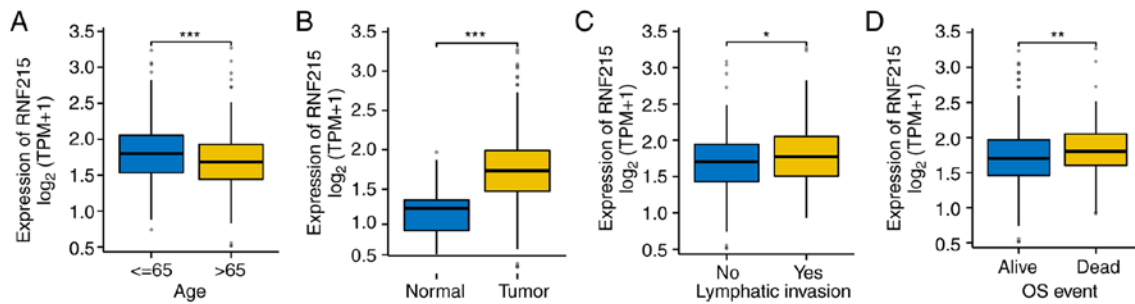
Figure 4. Associations between ring finger protein 215 expression and clinical characteristics. (A) Age. (B) Tumor vs. normal. (C) Lymphatic invasion. (D) Overall survival event. *P<0.05, **P<0.01 and ***P<0.001. RNF215, ring finger protein 215; OS, overall survival.
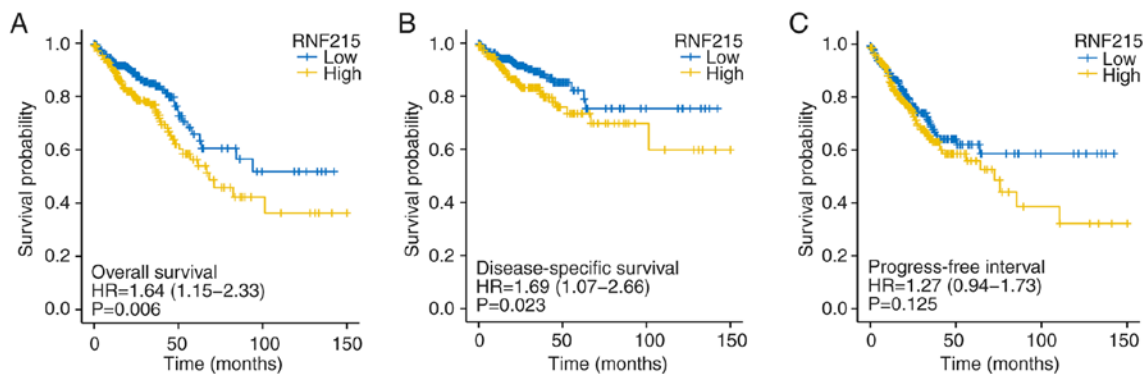

Figure 5. Survival analysis of RNF215 in colorectal cancer. OS, DSS and PFI curves of patients with high vs. low RNF215 expression levels. (A) OS. (B) DSS. (C) PFI. RNF215, ring finger protein 215; OS, overall survival; DSS, disease-specific survival; PFI, progression-free interval.

probability was constructed to assess the consistency between the predicted OS and the actual OS, and it suggested that the nomogram prediction was credible (Fig. 6B).

GO and KEGG analyses and PPIs. The function of RNF215 was predicted by GO and KEGG analyses using the R package clusterProfiler (version, 3.14.3) (13). According to cutoffs of a

Table II. Univariate and multivariate analysis of clinicopathological characteristics that are correlated with the overall survival of patients with colorectal cancer.

Characteristics	Total (N)	Univariate analysis		Multivariate analysis	
		Hazard ratio (95% CI)	P-value	Hazard ratio (95% CI)	P-value
T stage (T1 and T2 vs. T3 and T4)	640	2.468 (1.327-4.589)	0.004	2.248 (1.017-4.967)	0.045
N stage (N0 vs. N1 and N2)	639	2.627 (1.831-3.769)	<0.001	0.527 (0.201-1.382)	0.193
M stage (M0 vs. M1)	563	3.989 (2.684-5.929)	<0.001	2.492 (1.540-4.033)	<0.001
Pathologic stage (stage I and II vs. stage III and IV)	622	2.988 (2.042-4.372)	<0.001	4.142 (1.417-12.104)	0.009
Age (>65 vs. ≤65)	643	1.939 (1.320-2.849)	<0.001	3.179 (2.027-4.986)	<0.001
Sex (female vs. male)	643	1.054 (0.744-1.491)	0.769		
Primary therapy outcome (PD and SD vs. PR and CR)	312	0.109 (0.058-0.202)	<0.001	0.084 (0.023-0.314)	<0.001
BMI (≥25 vs. <25)	329	0.649 (0.394-1.069)	0.090	1.701 (0.351-8.235)	0.509
Residual tumor (R0 vs. R1 and R2)	509	4.609 (2.804-7.577)	<0.001	14.670 (1.230-174.902)	0.034
CEA level (≥5 vs. <5)	414	2.620 (1.611-4.261)	<0.001	1.840 (0.817-4.145)	0.141
Perineural invasion (positive vs. negative)	235	1.692 (0.907-3.156)	0.099	1.496 (0.636-3.520)	0.356
Lymphatic invasion (positive vs. negative)	581	2.144 (1.476-3.114)	<0.001	2.561 (1.093-6.002)	0.030
Location (colon vs. rectum)	643	0.799 (0.519-1.230)	0.308		
RNF215 (low vs. high)	643	1.641 (1.154-2.334)	0.006	1.859 (1.254-2.755)	0.002

RNF215, ring finger protein 215.

P.adj <0.05 and q-value <0.2, the 96 GO/KEGG items were divided into four groups: The biological process (BP) group (74 items), the cellular component (CC) group (9 items), the molecular function (MF) group (7 items), and the KEGG group (6 items); the details are presented in Table SIII. GO term analysis for the BP category suggested that 'nucleosome organization', 'chromatin assembly', and 'nucleosome assembly' were positively enriched. GO term analysis for the CC category showed that the 'protein-DNA complex assembly', 'DNA packaging complex', and 'nucleosome' were positively enriched. The MF analysis showed that 'taste receptor activity', 'bitter taste receptor activity', and 'nucleosomal DNA binding' were positively enriched. KEGG analysis suggested that 'alcoholism', 'systemic lupus erythematosus', and 'viral carcinogenesis' were the most positively enriched pathways. All the significant GO/KEGG pathways are presented in Fig. 7A and B, and the GO/KEGG results combined with the logFC results are shown in Fig. 7C and D.
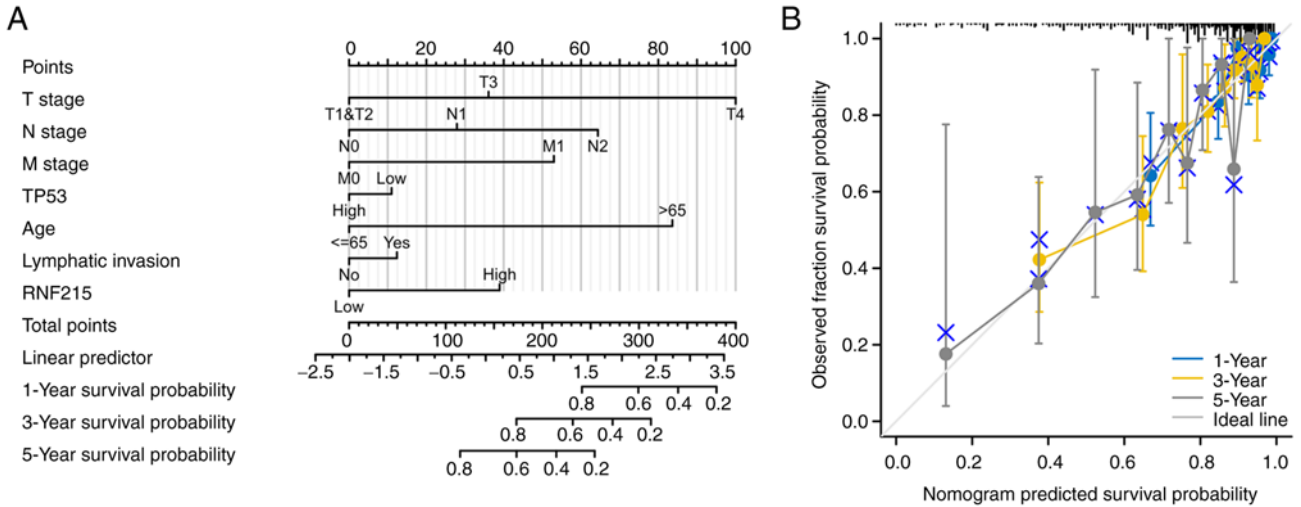
Figure 6. Nomogram and calibration curve. (A) Nomogram for predicting the probability of 1-, 3-, and 5-year OS for colorectal cancer patients. T stage, N stage, M stage, TP53 status, age, lymphatic invasion, and ring finger protein 215 expression were selected for inclusion in the nomogram. (B) Calibration curve of the nomogram for predicting the probability of OS at 1, 3, and 5 years, indicating the credibility of the prediction. OS, overall survival; RNF215, ring finger protein 215.
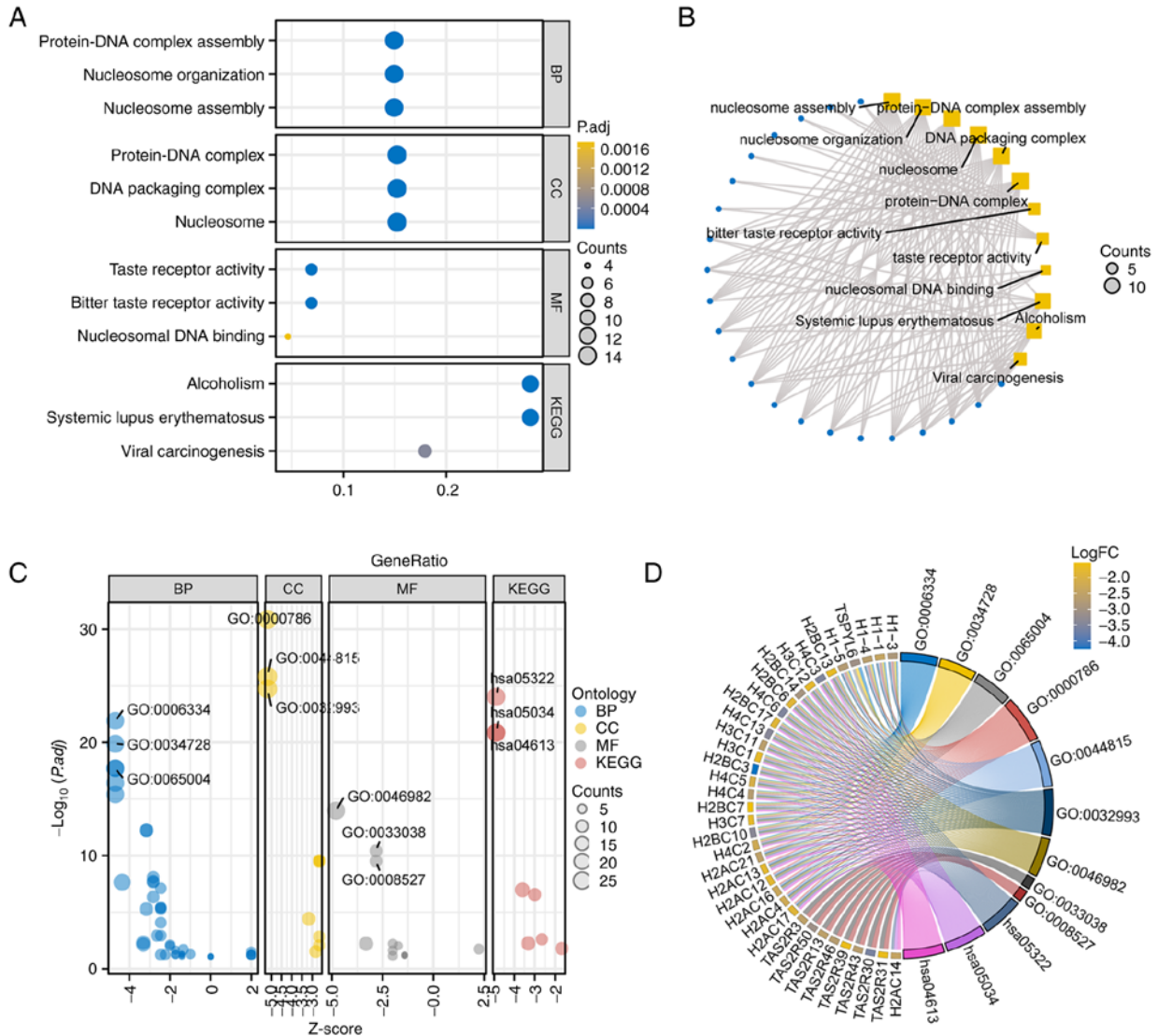

Figure 7. Enrichment analysis of ring finger protein 215 and neighboring genes. (A) Bubble diagram from GO/KEGG analysis. (B) Visual networks analyzed using GO/KEGG. (C) Bubble diagram from GO/KEGG combined with logFC analysis. (D) Circle diagram from GO/KEGG combined with logFC analysis. GO, Gene Ontology; KEGG, Kyoto Encyclopedia of Genes and Genomes.
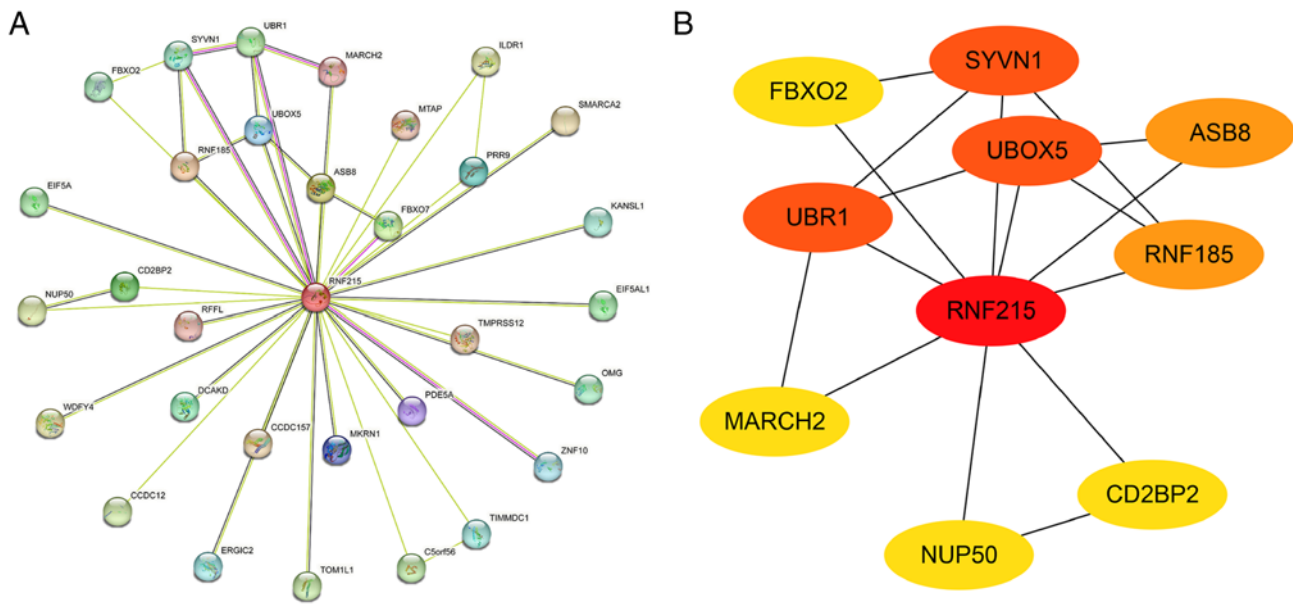
Figure 8. Protein-protein interaction network. (A) RNF215-interacting proteins according to the STRING tool. (B) RNF215 and the top nine most associated proteins according to cytoHubba using Cytoscape. The node color reflects the degree of connectivity (red color represents a higher degree, and yellow color represents a lower degree). RNF215, ring finger protein 215.

To further identify the possible molecular role of RNF215 in tumorigenesis, the known RNF215-interacting proteins and expression-correlated genes were filtered out with the STRING tool (Fig. 8A). Subsequently, a second network was constructed using the tsv file and input in Cytoscape (version, 3.9.1). The top nine hub genes obtained by the maximal clique centrality (MCC) methods (one of the algorithms in the plug-in Cytohubba) and according to the node degree was screened, including FBXO2, SYVN1, UBR1, UBOX5, ASB8, RNF185, MARCH2, NUP50, and CD2BP2, as shown in Fig. 8B. Therefore, RNF215 may participate in tumorigenesis by interacting with these proteins.

GSEA. To investigate the signaling pathways differentially activated in CRC, GSEA was then performed on the basis of the RNF215 low- and high-expression datasets. A total of 318 items satisfied the conditions of an FDR <0.25 and a P.adj <0.05. GSEA suggested that RNF215 was involved in several key pathways and biological processes associated with tumor occurrence, including the KEGG MAPK signaling pathway (NES=1.609, P.adj=0.024, FDR=0.020), the WP RAS signaling pathway (NES=1.624, P.adj=0.024, FDR=0.020), the WP PI3KAKT signaling pathway (NES=1.754, P.adj=0.024, FDR=0.020), KEGG pathways in cancer (NES=1.707, P.adj=0.024, FDR=0.020), KEGG melanogenesis (NES=1.573, P.adj=0.031, FDR=0.026), the WP WNT signaling pathway (NES=1.797, P.adj=0.024, FDR=0.020), and Reactome signaling by MET (NES=1.575, P.adj=0.042, FDR=0.034) (Fig. 9A-G). Reactome DNA methylation (NES=-3.338, P.adj=0.024, FDR=0.020) and KEGG propanoate metabolism (NES=-1.681, P.adj=0.036, FDR=0.030) were also identified (Fig. 9H and I). The results revealed that RNF215 may contribute to the development of CRC progression by participating in some CRC-associated signaling pathways. The detailed GSEA results are shown in Table SIV.

Correlation of RNF215 expression and immune cell infiltration levels in CRC. The relationship between RNF215 and 24 immune cell infiltrates quantified by ssGSEA in the CRC microenvironment of tumors were investigated using Spearman's correlation analysis (Fig. 10A). RNF215 expression showed a positive linear correlation with the infiltration levels of natural killer (NK) cells (r=0.401, P<0.001), CD8 T cells (r=0.242, P<0.001), Tregs (r=0.245, P<0.001; Fig. 10A-F). RNF215 expression was also negatively correlated with infiltration of T helper cells (R=-0.149, P<0.001; Fig. 10G). These results revealed that RNF215 may regulate immune cell infiltration in CRC tumors.

Analysis of RNF215 expression and angiogenesis. To further clarify the association between RNF215 and angiogenesis, a coexpression analysis between RNF215 and angiogenesis-associated markers in CRC was performed using the TCGA dataset, as shown in Fig. 11A. In addition, 36 angiogenesis-associated genes were acquired from the MSigDB Team (Hallmark gene set); the details are shown in Table SV. The present study confirmed that many of the genes involved in angiogenesis (such as APP, COL3A1, JAG2, PDGFA, S100A4, and VEGFA) were consistent with the trend in RNF215 expression in CRC. The immunohistochemical results indicated that RNF215 was present in the vascular tissues around CRC tumors (Fig. 11B and C), indicating that RNF215 may be involved in angiogenesis in CRC.

Validation of RNF215 expression by IHC. IHC was performed on 177 CRC tumor and corresponding normal tissues obtained from the Department of Pathology, Shanghai Fifth People's Hospital, Fudan University. Representative images of RNF215 expression are shown in Fig. 12A-C. The results indicated that RNF215 expression was higher in CRC tissues than in corresponding normal tissues (P<0.01), as shown in
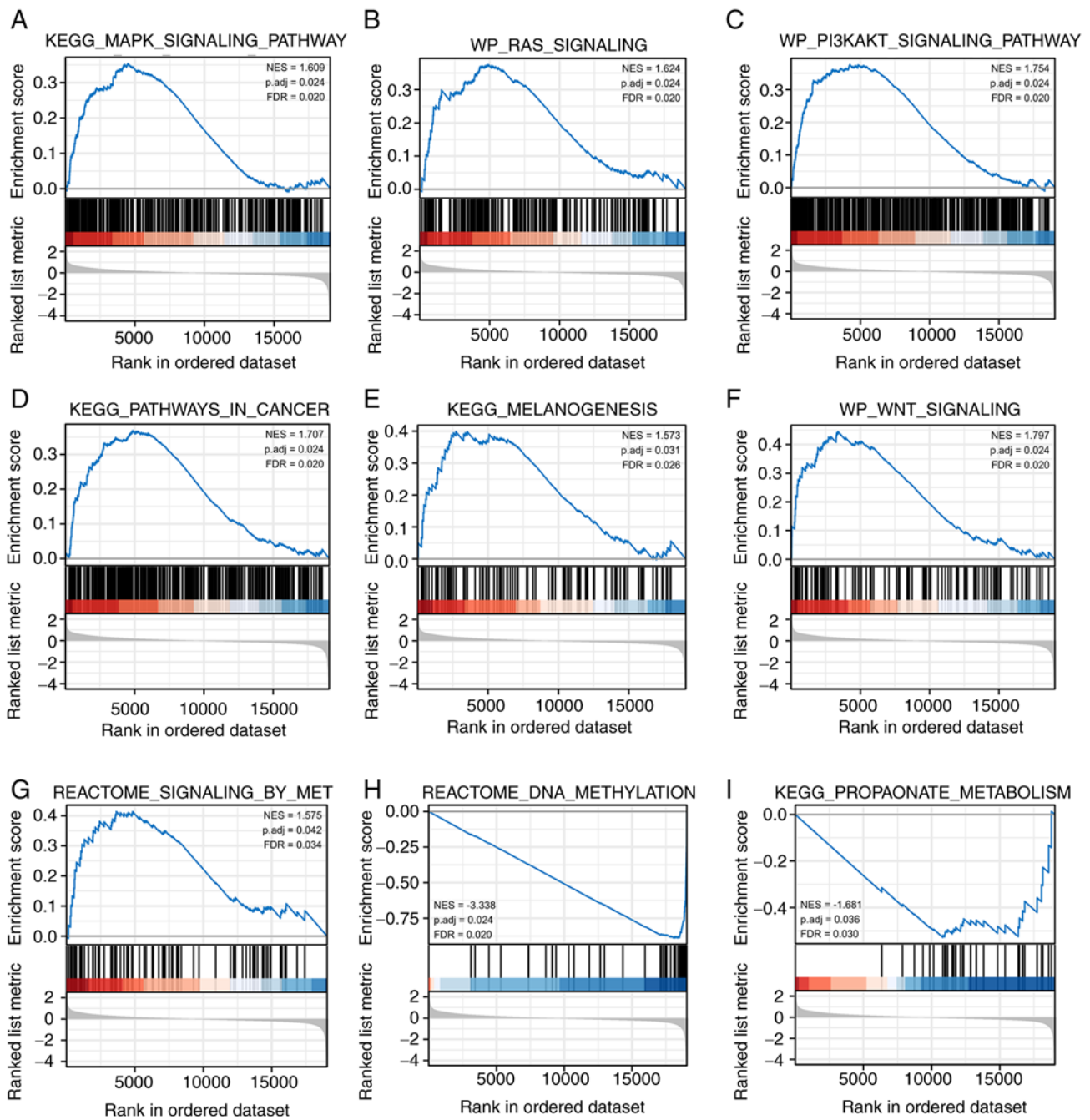
Figure 9. Enrichment plots from gene set enrichment analysis. Some items were enriched in ring finger protein 215-related colorectal cancer. (A) KEGG MAPK signaling pathway (NES=1.609, P.adj=0.024, FDR=0.020). (B) WP RAS signaling pathway (NES=1.624, P.adj=0.024, FDR=0.020). (C) WP PI3KAKT signaling pathway (NES=1.754, P.adj=0.024, FDR=0.020). (D) KEGG pathways in cancer (NES=1.707, P.adj=0.024, FDR=0.020). (E) KEGG melanogenesis (NES=1.573, P.adj=0.031, FDR=0.026). (F) WP WNT signaling pathway (NES=1.797, P.adj=0.024, FDR=0.020). (G) Reactome signaling by MET (NES=1.575, P.adj=0.042, FDR=0.034). (H) Reactome DNA methylation (NES=-3.338, P.adj=0.024, FDR=0.020). (I) KEGG propanoate metabolism (NES=-1.681, P.adj=0.036, FDR=0.030). KEGG, Kyoto Encyclopedia of Genes and Genomes; NES, normalized enrichment score; P.adj, adjusted P-value; FDR, false discovery rate.

Fig. 12D. Compared to patients with CRC with negative or weak RNF215 expression in the present study, patients with CRC with RNF215 overexpression were younger, had more lymphatic invasion, and had more distant metastases (P<0.05). Furthermore, patients with CRC with RNF215 overexpression had poorer OS and DFS than patients with CRC with negative or weak RNF215 expression (P<0.001), as revealed in Fig. 12E and F. The clinicopathological details of RNF215 expression in the patients with CRC are presented in Table III.

Discussion

RNF215 is a protein-coding gene located in the membrane or intracellularly. According to GeneCards (https://www.gene-cards.org/), RNF215 is predicted to have ubiquitin-protein ligase activity and is involved in Golgi to vacuolar transport, vacuolar protein targeting, and ubiquitin-dependent protein decomposition processes. It is also predicted to be an integral component of the cell membrane, to be part of the nuclear Golgi transport
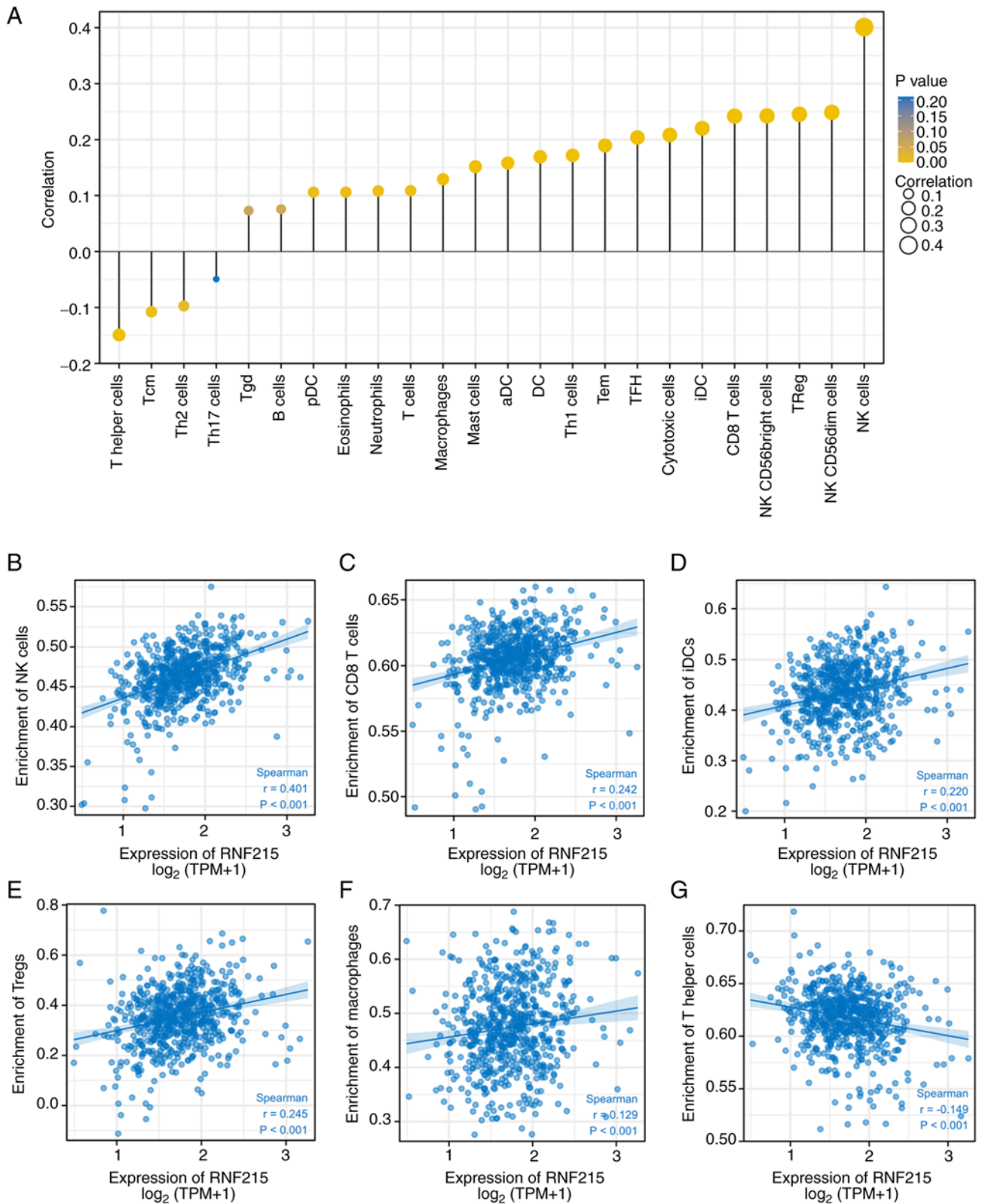
Figure 10. Correlation analysis between RNF215 expression and immune infiltration. (A) Association between RNF215 expression and 24 tumor-infiltrating lymphocytes. (B-G) Correlation of RNF215 expression with the immune infiltration levels of (B) natural killer cells, (C) CD8 T cells, (D) iDCs, (E) Tregs, (F) macrophages, and (G) T helper cells. RNF215, ring finger protein 215; NK, natural killer.

complex, and to be active in the endosomes, membranes, and trans-Golgi networks. To date, only a few studies have been reported on RNF215 (8-10); however, no studies have reported on the association between RNF215 and CRC.

In the present research, bioinformatics analysis indicated that the RNF215 expression value in CRC tumor tissues was higher than that in paired or unpaired normal tissues, suggesting that RNF215 may play an important role in CRC tumorigenesis
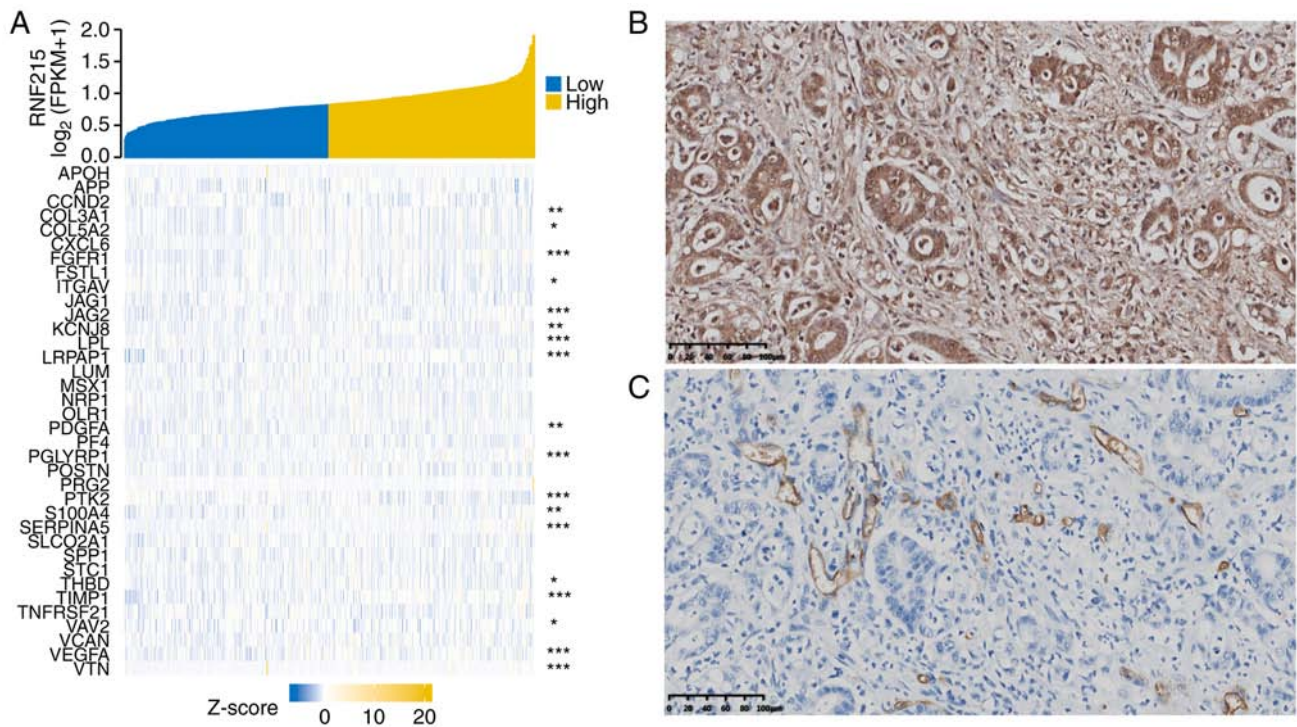
Figure 11. RNF215 and angiogenesis-associated genes. (A) Coexpression heatmap between RNF215 and 36 angiogenesis-associated genes. (B) Immunostaining of RNF215. (C) Immunostaining of CD34. *P<0.05, **P<0.01 and ***P<0.001. RNF215, ring finger protein 215.
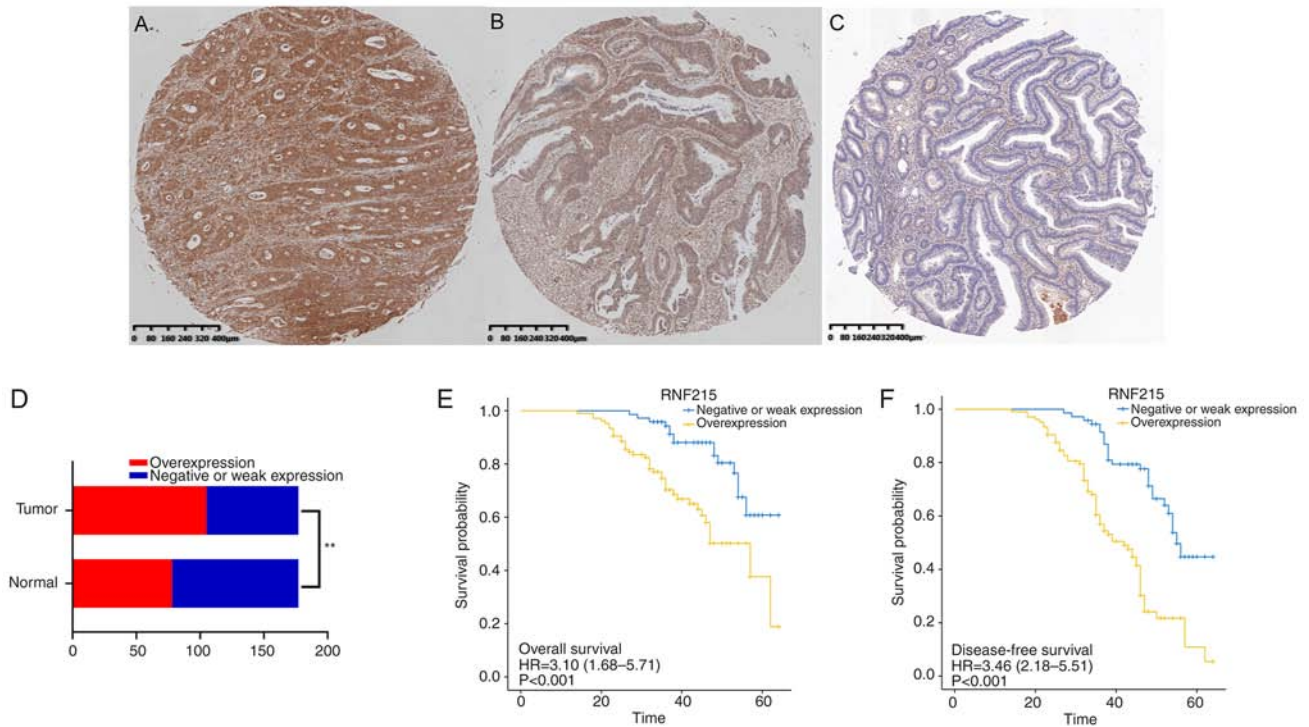

Figure 12. Validation of RNF215 expression using IHC in samples from patients with CRC. (A-C) Representative immunostaining images of (A) RNF215 overexpression, (B) weak RNF215 expression, and (C) negative RNF215 expression. (D) Comparison between RNF215 overexpression and negative or weak expression in CRC tumors and paired normal tissues. (E) Patients with RNF215 overexpression had significantly poorer overall survival than patients with negative or weak RNF215 expression. (F) Patients with RNF215 overexpression had significantly poorer disease-free survival than patients with negative or weak RNF215 expression. **P<0.01. RNF215, ring finger protein 215; OS, overall survival; DFS, disease-free survival.

and progression. Moreover, ROC analysis revealed that the AUC for CRC was 0.845, indicating that RNF215 may be a potential molecular biomarker. Therefore, the association

between RNF215 expression and clinicopathological features was further explored. High RNF215 expression was positively associated with age (P=0.001), lymphatic invasion (P=0.017),

Table III. Association between RNF215 expression and clinicopathological characteristics in patients with colorectal cancer.

Characteristics	Negative or low expression of RNF215	Overexpression of RNF215	P-value
n	72 (%)	105 (%)	
Sex, n (%)			0.3017
Male	50 (28.25)	65 (36.72)	
Female	22 (12.43)	40 (22.60)	
Age, n (%)			0.0381
≤65	25 (14.12)	53 (29.94)	
>65	47 (26.55)	52 (29.38)	
Localization, n (%)			0.4815
Right colon	27 (15.25)	34 (19.21)	
Left colon	45 (25.42)	71 (40.11)	
Configuration, n (%)			0.3046
Endophytic	48 (27.12)	62 (35.03)	
Exophytic	24 (13.56)	43 (24.29)	
Size, n (%)			0.2314
≤3.5 cm	13 (7.34)	27 (15.25)	
>3.5 cm	59 (33.33)	78 (44.07)	
Pathologic stage, n (%)			0.0793
Stage I-II	30 (17.88)	32 (17.88)	
Stage III-IV	42 (23.46)	73 (40.78)	
T stage, n (%)			
T1-T2	4 (2.26)	16 (9.04)	0.0543
T3-T4	68 (38.42)	89 (50.28)	
N stage, n (%)			0.7832
N0	44 (24.86)	62 (35.03)	
N1-N2	28 (15.82)	43 (24.29)	
M stage, n (%)			0.0026
M0	52 (29.38)	52 (29.38)	
M1	20 (11.30)	53 (29.94)	
Perineural invasion, n (%)			0.7759
Negative	50 (28.25)	75 (42.37)	
Positive	22 (12.43)	30 (16.95)	
Lymphatic invasion, n (%)			0.0325
Negative	48 (27.12)	53 (29.94)	
Positive	24 (13.56)	52 (29.38)	

RNF215, ring finger protein 215.

and OS (P=0.018). Since a role of RNF215 in CRC progression has not been reported, the clinical role of RNF215 has not been determined. The prognostic gene signature was first modeled according to the Kaplan-Meier curve of RNF215, which showed that it performed well in predicting CRC survival. The present study revealed poorer OS, DSS, and PFI in CRC patients with high RNF215 expression, although the PFI difference was not significant. In addition, the multivariate analysis suggested that RNF215 was an independent factor affecting CRC survival (P=0.002). According to the Cox proportional hazards regression results, the prognostic model had a C-index of 0.777 and was reliable. All these results

indicate that RNF215 may be a potential molecular biomarker of CRC.

To further investigate the potential value of RNF215 in CRC, GO and KEGG analyses and GSEA were conducted on RNF215. In GO analysis, BP terms associated with nucleosomes were identified, including 'nucleosome organization', 'nucleosome assembly', 'nucleosome', 'nucleosomal DNA binding' and 'DNA packaging complex'. KEGG analysis showed that 'alcoholism', 'systemic lupus erythematosus', and 'viral carcinogenesis' were the most significantly enriched pathways. Previous research has revealed that viral carcinogenesis may participate in the tumorigenesis

in numerous types of cancers, such as cervical and oropharyngeal cancers (24), Markel cell carcinoma, and Kaposi sarcoma (25). RNF215 coupled with its coexpressed genes may be involved in cell signaling and the viral oncogenic pathway, which in turn may be necessary for the tumorigenesis and development of CRC.

In GSEA, multiple pathways were positively enriched and associated with high RNF215 expression, including the KEGG MAPK signaling pathway, the WP RAS pathway, the WP PI3KAKT signaling pathway, and KEGG pathways in cancer. Slattery *et al* suggested that the MAPK signaling pathway is dysregulated in CRC (26). In addition, a study by Li *et al* has suggested that Mex3a promotes tumorigenesis via the RAP1/MAPK signaling pathway in CRC (27). Some other studies have investigated whether dysregulated signaling through RAS/RAF/MEK/ERK is a common event in CRC (28,29). Kasprzak *et al* indicated that the components of the IGF axis may interact directly or indirectly and that these interactions may be related to activation of the PI3K/Akt signaling pathway (30). Furthermore, it has been demonstrated that the ubiquitin ligase NEDD4 may be an oncogene in endometrial cancer and may stimulate activation of the IGF-1R/PI3K/Akt signaling pathway (31). Yi *et al* suggested that the frequently highly mutated genes in CRC liver metastases were mainly enriched in gastric acid secretion, biliary secretion, and melanogenesis (32). Overall, the data of the present study confirmed that RNF215 may be necessary for regulating CRC invasion; nevertheless, more research is required to further elucidate the possible modulatory mechanisms of RNF215 in CRC. In addition, nine top hub genes (FBXO2, SYVN1, UBR1, UBOX5, ASB8, RNF185, MARCH2, NUP50, and CD2BP2) were identified to be associated with RNF215 using STRING and Cytoscape software, suggesting that these genes may be involved in CRC carcinogenesis.

Some studies have suggested that the CRC microenvironment could contribute to changes in immunity during CRC development (33-35). In order to explore the immune infiltration in CRC, ssGSEA and Spearman's correlation analysis based on transcriptomic data was performed to evaluate the correlations of RNF215 with immune cell populations. The present study revealed that RNF215 expression was positively associated with immune cells, including NK cells, NK CD56dim cells, and neutrophils; these immune cells may play an important role in CRC tumorigenesis. Some researchers have postulated that the immune microenvironment and immune-related mechanisms of tumor cells are important components of tumor development and tumor treatment efficiency and are closely related to clinical efficacy (5,20). The findings from the present study demonstrated that RNF215 participates in the regulation of immune infiltrates in the local CRC microenvironment. However, a nonbiased approach is required to further analyze the role and pathway of RNF215 in CRC immune infiltration.

Another focus of the present research was to determine the role of RNF215 in CRC angiogenesis. The present study indicated that in CRC, RNF215 is highly coexpressed with multiple factors, including APP, COL3A1, JAG2, PDGFA, S100A4 and VEGFA, which have been confirmed to be necessary for angiogenesis in various tumors (36-38). The

immunohistochemical results revealed that RNF215 was present in the vascular tissues around colorectal tumors, suggesting a close association between RNF215 and vascular development. The angiogenic process of CRC is complex, and future studies need to further investigate the value of RNF215 in the targeted adjustment of angiogenesis in animal models.

To further verify the possible role of RNF215 in CRC, immunohistochemical analysis was carried out on samples from 177 patients with CRC from the Department of Pathology, Shanghai Fifth People's Hospital, Fudan University, and the association between RNF215 expression and clinicopathological features was estimated. The results revealed significant associations between RNF215 expression and age, lymphatic invasion, and metastasis, mostly in line with the TCGA results. The small differences may have been due to the number of cases or to differences in ethnicity and geographical location.

Although the present study, to the best of our knowledge is the first to investigate the correlation between RNF215 and CRC, there are still several limitations that need to be recognized. First, the main data in the research was obtained from TCGA, and immunohistochemical analysis was only conducted to validate the conclusions. Furthermore, *in vitro* and *in vivo* experimental studies are required. Second, the sample size of the present study was relatively small; a larger sample size is needed to improve the reliability of the results, which may affect the data on the expression of RNF215. Finally, the present research had limitations inherent to the retrospective research design. Thus, further prospective studies with large sample sizes are required to validate the results in the future.

In conclusion, in the present study, comprehensive bioinformatics analysis and immunohistochemical verification were mainly conducted. The findings of the present study indicated that high RNF215 expression is predictive of poor prognosis in CRC. RNF215 may become a novel biomarker for predicting poor prognosis and a molecular target for immunotherapy in CRC in the future. However, the study was limited by a small sample size and a lack of adequate experimental validation. Thus, studies with larger sample sizes as well as further cytological, histological, and experimental animal studies are required to confirm the findings of the present study.

Availability of data and materials

The public data of the study are available from TCGA (https://portal.gdc.cancer.gov/). The other data that support the findings of this study are available from the corresponding author upon reasonable request.

Authors' contributions

JBW conceptualized the study and its methodology and wrote and prepared the original draft. HL performed the immuno-histochemical experiments and data analysis. XJL curated the data and performed statistical analysis. XPL designed the study and revised the final manuscript. JBW and HL confirm the authenticity of all the raw data. All authors have read and approved the final manuscript.

Ethics approval and consent to participate

The studies involving human participants were reviewed and approved by the Ethical Committee of Shanghai Fifth People's Hospital, Fudan University, Shanghai, China (approval no. 2021071). The patients/participants provided their written informed consent to participate in this study.

Patient consent for publication

Not applicable.

Competing interests

The authors declare that they have no competing interests.

References

1. Sung H, Ferlay J, Siegel RL, Laversanne M, Soerjomataram I, Jemal A and Bray F: Global cancer statistics 2020: GLOBOCAN estimates of incidence and mortality worldwide for 36 cancers in 185 countries. CA Cancer J Clin 71: 209-249, 2021.
2. Xia C, Dong X, Li H, Cao M, Sun D, He S, Yang F, Yan X, Zhang S, Li N and Chen W: Cancer statistics in China and United States, 2022: Profiles, trends, and determinants. Chin Med J (Engl) 135: 584-590, 2022.
3. Chen W, Zheng R, Baade PD, Zhang S, Zeng H, Bray F, Jemal A, Yu XQ and He J: Cancer statistics in China, 2015. CA Cancer J Clin 66: 115-132, 2016.
4. Mattiuzzi C, Sanchis-Gomar F and Lippi G: Concise update on colorectal cancer epidemiology. Ann Transl Med 7: 609, 2019.
5. Shang Y, Zhang Y, Liu J, Chen L, Yang X, Zhu Z, Li D, Deng Y, Zhou Z, Lu B and Fu CG: Decreased E2F2 expression correlates with poor prognosis and immune infiltrates in patients with colorectal cancer. J Cancer 13: 653-668, 2022.
6. Simon K: Colorectal cancer development and advances in screening. Clin Interv Aging 11: 967-976, 2016.
7. Kasi PM, Shahjehan F, Cochuyt JJ, Li Z, Colibaseanu DT and Merchea A: Rising proportion of young individuals with rectal and colon cancer. Clin Colorectal Cancer 18: e87-e95, 2019.
8. Wu Y, Chen D, Hu Y, Zhang S, Dong X, Liang H, Liang M, Zhu Y, Tan C, An S, et al: Ring finger protein 215 negatively regulates type I IFN production via blocking NF-κB p65 activation. J Immunol 209: 2012-2021, 2022.
9. Ma J, Li R and Wang J: Characterization of a prognostic four-gene methylation signature associated with radiotherapy for head and neck squamous cell carcinoma. Mol Med Rep 20: 622-632, 2019.
10. McIntosh LA, Marion MC, Sudman M, Comeau ME, Becker ML, Bohnsack JF, Fingerlin TE, Griffin TA, Haas JP, Lovell DJ, et al: Genome-wide association meta-analysis reveals novel juvenile idiopathic arthritis susceptibility loci. Arthritis Rheumatol 69: 2222-2232, 2017.
11. Ritchie ME, Phipson B, Wu D, Hu Y, Law CW, Shi W and Smyth GK: limma powers differential expression analyses for RNA-sequencing and microarray studies. Nucleic Acids Res 43: e47, 2015.
12. Love MI, Huber W and Anders S: Moderated estimation of fold change and dispersion for RNA-seq data with DESeq2. Genome Biol 15: 550, 2014.
13. Yu G, Wang LG, Han Y and He QY: clusterProfiler: An R package for comparing biological themes among gene clusters. OMICS 16: 284-287, 2012.
14. Walter W, Sánchez-Cabo F and Ricote M: GOplot: An R package for visually combining expression data with functional analysis. Bioinformatics 31: 2912-2914, 2015.
15. Subramanian A, Tamayo P, Mootha VK, Mukherjee S, Ebert BL, Gillette MA, Paulovich A, Pomeroy SL, Golub TR, Lander ES and Mesirov JP: Gene set enrichment analysis: A knowledge-based approach for interpreting genome-wide expression profiles. Proc Natl Acad Sci USA 102: 15545-15550, 2005.
16. Shannon P, Markiel A, Ozier O, Baliga NS, Wang JT, Ramage D, Amin N, Schwikowski B and Ideker T: Cytoscape: A software environment for integrated models of biomolecular interaction networks. Genome Res 13: 2498-2504, 2003.
17. von Mering C, Huynen M, Jaeggi D, Schmidt S, Bork P and Snel B: STRING: A database of predicted functional associations between proteins. Nucleic Acids Res 31: 258-261, 2003.
18. Szklarczyk D, Gable AL, Nastou KC, Lyon D, Kirsch R, Pyysalo S, Doncheva NT, Legeay M, Fang T, Bork P, et al: The STRING database in 2021: Customizable protein-protein networks, and functional characterization of user-uploaded gene/measurement sets. Nucleic Acids Res 49 (D1): D605-D612, 2021.
19. Hänzelmann S, Castelo R and Guinney J: GSVA: Gene set variation analysis for microarray and RNA-seq data. BMC Bioinformatics 14: 7, 2013.
20. Bindea G, Mlecnik B, Tosolini M, Kirilovsky A, Waldner M, Obenauf AC, Angell H, Fredriksen T, Lafontaine L, Berger A, et al: Spatiotemporal dynamics of intratumoral immune cells reveal the immune landscape in human cancer. Immunity 39: 782-795, 2013.
21. Wu JB, Sarmiento AL, Fiset PO, Lazaris A, Metrakos P, Petrillo S and Gao ZH: Histologic features and genomic alterations of primary colorectal adenocarcinoma predict growth patterns of liver metastasis. World J Gastroenterol 25: 3408-3425, 2019.
22. Chaves FN, Bezerra TMM, Moraes DC, Costa SFDS, Silva PGB, Alves APNN, Costa FWG, Bernardes VF and Pereira KMA: Loss of heterozygosity and immunoexpression of PTEN in oral epithelial dysplasia and squamous cell carcinoma. Exp Mol Pathol 112: 104341, 2020.
23. Liu J, Lichtenberg T, Hoadley KA, Poisson LM, Lazar AJ, Cherniack AD, Kovatich AJ, Benz CC, Levine DA, Lee AV, et al: An integrated TCGA pan-cancer clinical data resource to drive high-quality survival outcome analytics. Cell 173: 400-416.e11, 2018.
24. Hoppe-Seyler K, Bossler F, Braun JA, Herrmann AL and Hoppe-Seyler F: The HPV E6/E7 oncogenes: Key factors for viral carcinogenesis and therapeutic targets. Trends Microbiol 26: 158-168, 2018.
25. Krump NA and You J: Molecular mechanisms of viral oncogenesis in humans. Nat Rev Microbiol 16: 684-698, 2018.
26. Slattery ML, Mullany LE, Sakoda LC, Wolff RK, Samowitz WS and Herrick JS: The MAPK-signaling pathway in colorectal cancer: Dysregulated genes and their association with MicroRNAs. Cancer Inform 17: 1176935118766522, 2018.
27. Li H, Liang J, Wang J, Han J, Li S, Huang K and Liu C: Mex3a promotes oncogenesis through the RAP1/MAPK signaling pathway in colorectal cancer and is inhibited by hsa-miR-6887-3p. Cancer Commun (Lond) 41: 472-491, 2021.
28. Stec R, Bodnar L, Charkiewicz R, Korniluk J, Rokita M, Smoter M, Ciechowicz M, Chyczewski L, Nikliński J, Kozłowski W and Szczylik C: K-Ras gene mutation status as a prognostic and predictive factor in patients with colorectal cancer undergoing irinotecan- or oxaliplatin-based chemotherapy. Cancer Biol Ther 13: 1235-1243, 2012.
29. Meador CB and Pao W: Old habits die hard: Addiction of BRAF-mutant cancer cells to MAP kinase signaling. Cancer Discov 5: 348-350, 2015.
30. Kasprzak A, Kwasniewski W, Adamek A and Gozdzicka-Jozefiak A: Insulin-like growth factor (IGF) axis in cancerogenesis. Mutat Res Rev Mutat Res 772: 78-104, 2017.
31. Zhang Y, Goodfellow R, Li Y, Yang S, Winters CJ, Thiel KW, Leslie KK and Yang B: NEDD4 ubiquitin ligase is a putative oncogene in endometrial cancer that activates IGF-1R/PI3K/Akt signaling. Gynecol Oncol 139: 127-133, 2015.

32. Yi H, Liao ZW, Chen JJ, Shi XY, Chen GL, Wu GT, Zhou DY, Zhou GQ, Huang JY, Lian L, *et al*: Genome variation in colorectal cancer patient with liver metastasis measured by whole-exome sequencing. J Gastrointest Oncol 12: 507-515, 2021.

33. Sharp SP, Avram D, Stain SC and Lee EC: Local and systemic Th17 immune response associated with advanced stage colon cancer. J Surg Res 208: 180-186, 2017.

34. Tse BCY, Welham Z, Engel AF and Molloy MP: Genomic, microbial and immunological microenvironment of colorectal polyps. Cancers (Basel) 13: 3382, 2021.

35. Wang W, Zhong Y, Zhuang Z, Xie J, Lu Y, Huang C, Sun Y, Wu L, Yin J, Yu H, *et al*: Multiregion single-cell sequencing reveals the transcriptional landscape of the immune microenvironment of colorectal cancer. Clin Transl Med 11: e253, 2021.

36. Zhang Y, Yang F, Peng X, Li X, Luo N, Zhu W, Fu M, Li Q and Hu G: Hypoxia constructing the prognostic model of colorectal adenocarcinoma and related to the immune microenvironment. Front Cell Dev Biol 9: 665364, 2021.

37. Krämer M, Plum PS, Velazquez Camacho O, Folz-Donahue K, Thelen M, Garcia-Marquez I, Wölwer C, Büsker S, Wittig J, Franitza M, *et al*: Cell type-specific transcriptomics of esophageal adenocarcinoma as a scalable alternative for single cell transcriptomics. Mol Oncol 14: 1170-1184, 2020.

38. Ambartsumian N, Klingelhöfer J and Grigorian M: The multifaceted S100A4 protein in cancer and inflammation. Methods Mol Biol 1929: 339-365, 2019.